

2003 Mars Exploration Rover Orbit Determination Using Δ VLBI Data

Brian M. Portock, Robert Haw, Louis A. D'Amario
Jet Propulsion Laboratory, California Institute of Technology,
Pasadena, CA 91109-8099

Extended Abstract

Introduction

The Mars Exploration Rover (MER) mission plans to launch two spacecraft, each containing one rover, and to deliver them to the surface of Mars allowing the rovers to explore the surface and collect science data. Each spacecraft must be delivered to enter the Mars atmosphere accurately in order to meet the physical requirements of the entry, descent, and landing system, meet the requirement of surface safety (i.e. safe surface terrain) and allow scientifically interesting landing sites to be selected. In the past, interplanetary missions have used two-way Doppler and ranging data along with small amounts of various other data types for interplanetary navigation, but the resurgence of the Δ VLBI system, for navigation use, has given the Mars Exploration Rover mission another option. The MER mission has baselined an intensive campaign of Δ VLBI measurements which make it possible to meet delivery accuracy requirements. The Δ VLBI data enables a higher accuracy Mars delivery than that of Doppler and range only. This allows smaller landing ellipses for science and a more robust entry, descent, and landing system. This paper will show the improvements to the atmospheric entry delivery accuracy due to the addition of Δ VLBI data to the standard Doppler and range tracking.

Data Type Comparison

Δ VLBI data measures components of the spacecraft's position that are orthogonal to the components measured by Doppler and range data, therefore adding valuable information to the estimation process. Doppler and range measure the line-of-sight components of position and velocity. The Δ VLBI data, for MER, is known as Delta Differenced One-way Range (Δ DOR). This data type employs two Deep Space Network (DSN) stations at different complexes to simultaneously receive tones (known as DOR tones) from the spacecraft followed by simultaneous observations of a quasar as a reference radio source. These observations are used to measure the angular difference between the spacecraft and the quasar in the plane-of-sky along the line between the two DSN complexes. This direction is orthogonal to the line-of-sight to the spacecraft. Exactly how the line-of-sight to the spacecraft relates to information about the trajectory depends on where the spacecraft is in its trajectory, but generally for Mars missions Doppler and range data supplies information in the spacecraft's trajectory plane. The manner in which the Δ DOR data relates to the trajectory depends on the trajectory and

the DSN complexes, or baselines, used in the measurement. Since Δ DOR measures the plane-of-sky position of the spacecraft along the baseline, the way in which that baseline relates to the trajectory differs. The usual DSN complex pairs used as baselines are Goldstone-Madrid and Goldstone-Canberra. The Goldstone-Madrid baseline (oriented East-West) primarily measures the right ascension component of the spacecraft corresponding to an in-plane component of the trajectory. By similar reasoning, the Goldstone-Canberra baseline (oriented North-South) primarily measures the declination component of the spacecraft corresponding to the out-of-plane component of the trajectory (for most Mars missions). The third possible baseline, Madrid-Canberra, represents the longest baseline for the DSN, but is rarely scheduled because of very brief overlapping view periods.

Δ DOR data is independent of spacecraft dynamics. It is not necessary to rely on dynamic models to infer position as is the case for Doppler and range. The Δ DOR observable is a phase delay time expressed in units of nanoseconds (ns) that is equivalent to an angular separation between the spacecraft and the quasar. For the DSN, a delay of 1 ns corresponds to about 37.5 nanoradians (nrad) of angular displacement. Knowing the quasar's angular position determines a component of the spacecraft's position in plane-of-the-sky. By taking another measurement with an almost perpendicular baseline determines a second component.

Orbit Determination Process and Assumptions

Orbit determination (OD) processing is accomplished with a multiple batch consider-parameter filter, incorporating a baseline data set consisting of two-way coherent Doppler, two-way coherent ranging data, and Δ DOR measurements.

All trajectory correction maneuvers (TCMs) contained within the data arc are estimated. Future TCMs (i.e., with respect to a given data cutoff time) are treated in one of two ways. For generating entry delivery uncertainties, the TCM directly after the data cutoff time is considered in the filter at the a priori uncertainty, while any other future TCMs are ignored. For generating orbit determination covariances for maneuver analyses, all future TCMs are ignored, and maneuver execution errors are modeled in the maneuver analysis process.

Spacecraft attitude control system (ACS) Δ V events (e.g., spacecraft turns for attitude maintenance) are estimated in the OD filter when these events fall within the data arc, and they are considered at all times when the ACS event schedule places them in the future (i.e., between the end of the data arc and Entry). Each Δ V from an ACS event is modeled with a three-component impulse.

The solar pressure model consists of four components. For navigation analyses, however, only a single component (the solar array component) is estimated in the filter. This strategy is believed prudent, because the alternate choice of increasing the filter's

complexity by estimating all four solar pressure components does not elicit any greater insight or accuracy.

Stochastically estimated parameters include Earth orientation parameters, media effects, and Doppler and range data biases. The data biases are estimated during each tracking pass. Moreover, dynamic model margin has been incorporated to account for non-gravitational acceleration mis-modeling. A single, three-component stochastic acceleration is estimated along the trajectory for this purpose.

The considered parameters consist of quasar locations, station locations (a correlated 9x9 error covariance), and the Earth and Mars ephemerides. Considering these parameters (especially the quasar locations) is conservative, but is judged prudent in the absence of real data.

The combined effect of orbit determination errors and maneuver execution errors mapped to the atmospheric entry interface point is referred to in this document as the delivery accuracy. TCMs 4, 5, and 6 during the Approach phase are the key maneuvers used to target to the desired atmospheric entry interface conditions. The entry interface conditions consist of inertial entry flight path angle (FPA), B-plane angle, and time at the entry interface point, defined as Mars radius equal to 3522.2 km (see Figure 1). These conditions can also be met by targeting a B-plane aimpoint (B•T, B•R) along with a time of flight.

The entry interface conditions are derived from the desired landing target based

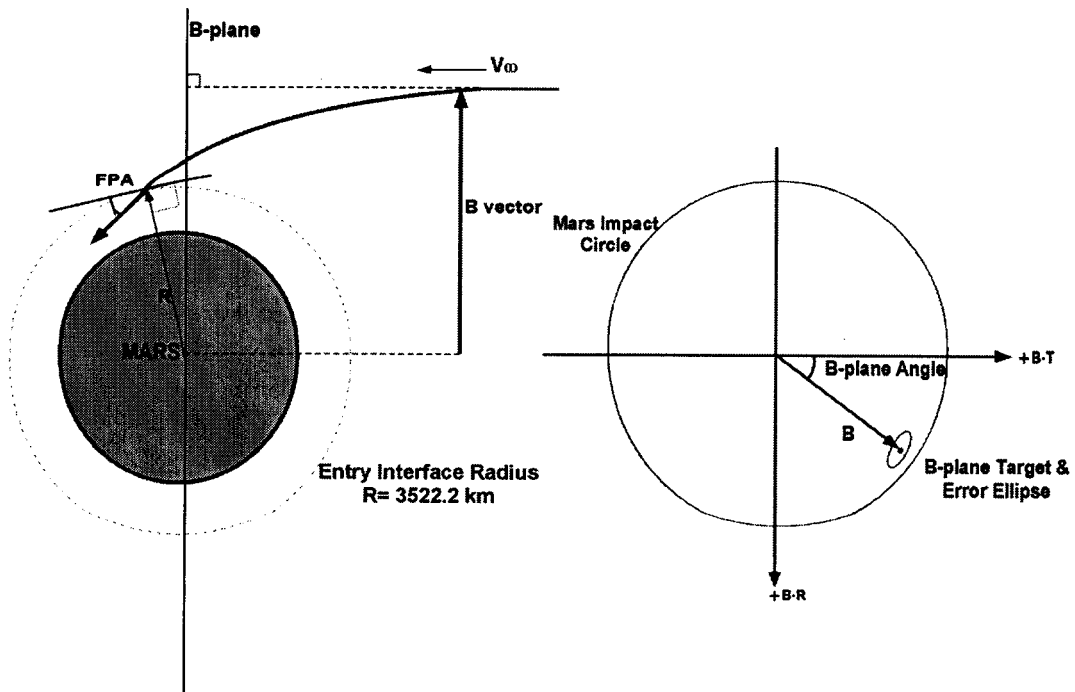


Figure 1. Entry Interface Diagram

on the trajectory of the spacecraft during the entry, descent and landing (EDL) phase. Targeting a specific B-plane angle and entry time corresponds to targeting latitude and longitude on the surface. The entry FPA is a parameter that affects the ballistic trajectory of the EDL system through the atmosphere. The atmospheric trajectory, and therefore, entry FPA, are constrained by the limits of the flight system. The flight system is designed for an entry FPA of $-11.5 \text{ deg} \pm 0.55 \text{ deg}$ (3σ). There is a tighter requirement on the FPA uncertainty due to landing ellipse size. The FPA uncertainty is the error source that drives the size of the landing ellipse. The landing ellipse sizes range in semi-major axis from 80 km to 340 km (3σ) corresponding to FPA uncertainty requirements ranging from 0.17 deg to 0.25 de (3σ), depending on the latitude of the landing site.

Table 1 presents a summary of the OD filter assumptions and error sources for the orbit determination results presented in the sections that follow. ACS events (i.e., spacecraft attitude maneuvers and thruster firings for spin-rate control) are included throughout the interplanetary trajectory at the frequency specified in Table 1. The ΔV from each ACS event in the data arc was estimated; the ΔV from each ACS event beyond the data cutoff was considered. The tracking data assumptions are shown in Table 2 for ΔDOR and Table 3 for Doppler and range.

Table 1 Baseline Orbit Determination Error Assumptions

Error Source	Estimated?	A Priori Uncertainty (1σ)	Correlation Time	Update Time	Comments/References
2-way Doppler (mm/s)	Ġ	0.075	Ġ	Ġ	~4.5 mHz
Range (m)	Ġ	4	Ġ	Ġ	29 range units
ÆDOR (nrad)	Ġ	4.5	Ġ	Ġ	0.12 ns
ÆDOR Schedule	Level 2 ^d				Level 2 (DSN request) with last point of final baseline pair no later than 2 days before data cutoff.
Epoch State					
Position (km)	√	1000	Ġ	Ġ	
Velocity (km/s)	√	1	Ġ	Ġ	
Range Bias (m)	√	2	0	Per pass	Estimated per pass.
Doppler Bias (mm/s)	√	0.005	0	Per pass	Estimated per pass.
Mars & Earth Ephemerides		DE405+	Ġ	Ġ	
Station Locations (cm)		3	Ġ	Ġ	
Pole X, Y (cm)	√	2 → 10	0	6 hrs	*Use lower value up to 7 days before data cutoff; then ramp up to higher value at data cutoff. (For UT1, 0.256 ms ⇒ ~10 cm.)
UT1 (cm)	√	2 → 10	0	6 hrs	
Quasar Locations (nrad)		2	Ġ	Ġ	
Ionosphere Ġ day (cm)	√	55	0	6 hrs	S-band values.
Ionosphere Ġ night (cm)	√	15	0	6 hrs	
Troposphere Ġ wet (cm)	√	1	0	6 hrs	
Troposphere Ġ dry (cm)	√	1	0	6 hrs	
Solar Pressure	Sunlit area of spacecraft.				
Area (%)	√	5	Ġ	Ġ	
ACS Event ÆV (mm/s)	Every 8 days				
Line-of-Sight Comp.	√	3	Ġ	Ġ	
Lateral Comp.	√	3	Ġ	Ġ	
Normal Comp.	√	3	Ġ	Ġ	
TCMs	Spherical uncertainty (mm/s).				
TCM-1	√	422, 440	Ġ	Ġ	MER-A Open Melas (VM53A), MER-B Open Hematite (TM20B)
TCM-2	√	17, 15	Ġ	Ġ	
TCM-3	√	3, 5	Ġ	Ġ	TCM-4 at E - 8 days TCM-5 at E - 2 days TCM-6 at E - 6 hrs (no TCM-5)
TCM-4	√	3, 3	Ġ	Ġ	
TCM-5	√	3, 3	Ġ	Ġ	5% (3σ) proportional error (per axis) 6 mm/s (3σ) fixed error (per axis)
TCM-6	√	7, 7	Ġ	Ġ	
Non-gravitational Accelerations (km/s ²)	√	2.0×10^{-12}	10 days	1 day	Spherical covariance. Estimated daily (1 day batches).

Table 2. Definitions of Δ DOR Frequency Levels

Relative Time (days)		Frequency of Δ DORs			
		DSN Request	Level 1	Level 2 (Baseline)	Level 3
Start	End				
L + 14	E - 45	1/week	1 every other week	1/week	1/week
E - 45	E - 28	2/week	1/week	2/week	2/week
E - 28	E - 8	1 every other day	2/week*	1 every other day*	1 every day*
E - 8	Entry	1/day	2/week*	1 every other day*	1 every day*

*Last Δ DOR point of final baseline pair no later than 2 days before data cutoff.

Table 3. Navigation Tracking Coverage (“DSN Request” and “Navigation Analysis”)

MER-A Open: Doppler and Range Coverage
Launch Date = 5/30/03, Arrival Date = 1/4/04

Relative Time (days)		Date		Doppler and Range Coverage	
Start	End	Start	End	DSN Request	Baseline Navigation Analysis
Launch	L + 30	5/30/03	6/29/03	Continuous	Continuous to L + 15 days; 2 tracks/day thereafter
L + 30	E - 45	6/29/03	11/20/03	3 tracks/week	3 tracks/week
E - 45	E - 21	11/20/03	12/14/03	~2.5 tracks/day	2 tracks/day
E - 21	Entry	12/14/03	1/4/04	Continuous	2 tracks/day

Results

The results in Tables 4 and 5 below are based on the process and assumptions described above. These results address two main topics. The first set of results in Table 4 show the improvement in the overall delivery accuracy due to the addition of Δ DOR data to Doppler and range data. Table 4 also shows the effect on the delivery accuracy from different levels or frequency of Δ DOR points. Table 5 shows the effect of varying the amount of Doppler and range tracking when a given amount of Δ DOR data is assumed.

The delivery results for variations in the Δ DOR frequency are given in Table 4. Addition of Δ DOR to the Doppler and range data provides a significant improvement to delivery accuracy from each maneuver. This improvement in delivery accuracy adds robustness to the design of the EDL system as well as allow for small landing ellipses on the surface. The greater the number of Δ DOR points acquired, the greater is the improvement as compared to the solution assuming Doppler and range data only. However, once a threshold is reached with the frequency of Δ DOR measurements, there is little additional improvement. One reason for this is the method used for simulating Δ DOR data. The data schedule is generated by first determining the time that is 48 hours (nominal Δ DOR latency time) before the data cut-off time before a given maneuver. Then working backwards in time, two consecutive Δ DOR points are scheduled (1 East/West baseline and 1 North /South baseline). From that point back to the beginning of the data arc, the appropriate Δ DOR schedule is followed for any given Δ DOR “level” as shown in Table 2. Therefore, before each maneuver, for any level of Δ DOR, there are always two points (one from each baseline) approximately 48 hours before the data cut-off. This attribute tends to lessen the impact of a reduced frequency of Δ DOR points. The overall improvement from a higher frequency of Δ DOR points (beyond the level at which delivery accuracy shows substantial improvement) is in the robustness of the navigation design to measurement failures.

The sensitivity to DSN coverage during the Approach Phase is shown in Table 5. In the presence of Δ DOR data, delivery accuracy is less sensitive to variations in Doppler and range coverage. Table 5 shows that decreasing the Doppler and range tracking by 50% has an appreciable negative impact on delivery errors. An increase to continuous coverage, on the other hand, produces little improvement. This shows that some coverage may be reduced to help alleviate the burden on the DSN complexes, but by reducing the coverage to only one track per day does have a negative impact on the accuracy.

Table 4. TCMs 4,5, and 6 Delivery Accuracy (3 σ)
 \square DOR Frequency = Doppler and Range Only, Level 1, or Level 3 (See Table 2)
(Mars-centered, Mars Mean Equator of Date)

	MER-A Open Melas (VM53A)				MER-B Open Hematite (TM20B)			
	Δ DOR Frequency				Δ DOR Frequency			
	Doppler & Range Only	Level 1	Baseline Level 2	Level 3	Doppler & Range Only	Level 1	Baseline Level 2	Level 3
TCM-4 Delivery (3σ) @ E – 8 days:								
Semi-major Axis (km)	46.2	17.2	16.8	16.1	27.1	18.1	17.8	17.6
Semi-minor Axis (km)	12.4	10.2	10.1	10.1	12.1	11.2	11.2	11.2
Ellipse Orientation Angle (deg)	91.5	112.0	112.0	112.0	98.8	109.4	109.3	110.1
Entry Time (s)	10.1	8.8	8.8	8.7	11.6	9.1	9.0	9.0
B Magnitude (km)	14.6	10.5	10.4	10.3	12.4	12.0	11.9	11.9
Flight Path Angle (deg)	± 0.58	± 0.42	± 0.41	± 0.41	± 0.50	± 0.49	± 0.48	± 0.49
TCM-5 Delivery (3σ) @ E – 2 days:								
Semi-major Axis (km)	21.4	10.8	10.7	9.9	15.4	11.0	10.5	10.4
Semi-minor Axis (km)	6.1	3.7	3.6	3.5	4.4	3.4	3.4	3.3
Ellipse Orientation Angle (deg)	95.4	112.0	113.0	112.0	101.3	107.7	107.2	107.0
Entry Time (s)	3.9	3.2	3.2	3.0	5.3	3.8	3.6	3.6
B Magnitude (km)	6.5	4.1	4.1	3.9	5.0	4.4	4.2	4.2
Flight Path Angle (deg)	± 0.26	± 0.16	± 0.16	± 0.15	± 0.20	± 0.18	± 0.17	± 0.17
TCM-6 Delivery (3σ) @ E – 6 hrs:								
Semi-major Axis (km)	11.1	11.0	9.5	8.5	8.8	7.8	7.3	6.8
Semi-minor Axis (km)	1.5	1.4	1.4	1.4	1.9	1.9	1.9	1.9
Ellipse Orientation Angle (deg)	118.0	118.0	118.0	117.0	115.4	115.5	115.4	115.4
Entry Time (s)	2.8	2.8	2.4	2.1	2.6	2.4	2.5	2.2
B Magnitude (km)	3.5	3.5	3.0	2.6	3.9	3.6	3.4	3.2
Flight Path Angle (deg)	± 0.14	± 0.14	± 0.12	± 0.11	± 0.16	± 0.15	± 0.14	± 0.13

Notes: 1. TCM-6 results assume TCM-5 does not occur.
2. Frequency of Δ DOR measurements for Level 1, Level 2, and Level 3 are given in Table 2.

Table 5. TCMs 4,5, and 6 Delivery Accuracy (3σ)
Doppler and Range Coverage =50%Baseline (1 track/day) or
150%Baseline (3 tracks/day)
(Mars-centered, Mars Mean Equator of Date)

	MER-A Open Melas (VM53A)			MER-B Open Hematite (TM20B)		
	Doppler and Range Coverage			Doppler and Range Coverage		
	50% 1 trk/day	Baseline 2 trks/day	150% 3 trks/day	50% 1 trk/day	Baseline 2 trks/day	150% 3 trks/day
TCM-4 Delivery (3σ) @ E – 8 days:						
Semi-major Axis (km)	17.5	16.8	16.1	18.6	17.8	17.4
Semi-minor Axis (km)	10.3	10.1	10.1	11.2	11.2	11.1
Ellipse Orientation Angle (deg)	113.0	112.0	111.0	109.6	109.3	108.8
Entry Time (s)	8.9	8.8	8.7	9.2	9.0	9.0
B Magnitude (km)	10.7	10.4	10.3	12.1	11.9	11.8
Flight Path Angle (deg)	±0.43	±0.41	±0.41	±0.49	±0.48	±0.48
TCM-5 Delivery (3σ) @ E – 2 days:						
Semi-major Axis (km)	11.6	10.7	10.1	11.8	10.5	10.4
Semi-minor Axis (km)	3.7	3.6	3.5	3.6	3.4	3.3
Ellipse Orientation Angle (deg)	113.0	113.0	111.0	108.4	107.2	106.8
Entry Time (s)	3.3	3.2	3.0	4.0	3.6	3.7
B Magnitude (km)	4.4	4.1	3.9	4.8	4.2	4.2
Flight Path Angle (deg)	±0.17	±0.16	±0.15	±0.20	±0.17	±0.17
TCM-6 Delivery (3σ) @ E – 6 hrs:						
Semi-major Axis (km)	10.2	9.5	9.1	9.3	7.3	7.3
Semi-minor Axis (km)	1.4	1.4	1.3	2.0	1.9	1.9
Ellipse Orientation Angle (deg)	118.0	118.0	117.0	115.6	115.4	115.4
Entry Time (s)	2.6	2.4	2.3	2.7	2.5	2.5
B Magnitude (km)	3.2	3.0	2.8	4.1	3.4	3.4
Flight Path Angle (deg)	±0.13	±0.12	±0.11	±0.17	±0.14	0.14

Notes: 1. TCM-6 results assume TCM-5 does not occur.

Conclusions

In order to meet the stringent Mars atmospheric entry delivery requirements MER has baseline the use of Δ DOR measurements in addition to standard Doppler and range data. The overall improvement in the FPA uncertainty due to Δ DOR ranges from 10% to 40% depending upon the landing site. The addition of Δ DOR also reduces the delivery accuracy sensitivity dues to variations in the amount Doppler and range data.